ADVANCED FUNCTIONAL MATERIALS

Supporting Information

for *Adv. Funct. Mater.,* DOI: 10.1002/adfm.202111242

Effect of the Threshold Kinetics on the Filament Relaxation Behavior of Ag-Based Diffusive Memristors

Solomon Amsalu Chekol, Stephan Menzel, Rana Walied Ahmad, Rainer Waser, and Susanne Hoffmann-Eifert**

Supporting Information

Effect of the Threshold Kinetics on the Filament Relaxation Behavior of Ag-Based Diffusive Memristors

*Solomon Amsalu Chekol, Stephan Menzel, Rana Walied Ahmad, Rainer Waser, and Susanne Hoffmann-Eifert**

1.1. Filament growth and the role of on-state current

The electrical connection through the conductive filament can be achieved in either a tunneling gap or galvanic contact, depending on the device structure and operational current range. To investigate this, the device was switched under various I_{CC} levels of 100 nA, 1 μA, 10 μA, and 100 μA (Figure S5). At lower I_{CC} of 100 nA and 1 μA, the conductance is given as $G << 1 \cdot G_0$ ($G_0 = 2e^2/h \approx 77.5\ \mu S \approx 12.9\ k\Omega^{-1}$, e electron charge and h Planck's contact), suggesting that the current increase is due to the tunneling of carriers through a small tunneling gap Figure S5a. As I_{CC} increases to 10 μA, a quantum conductance plaque of $< 1.5 \cdot G_0$ can be seen, indicating the contact formation between the thin conductive filament and the electrode (Figures S5b and c). Further increment of I_{CC} to 100 μA leads to a higher conductance of $6 \cdot G_0$ (Figure S5d).

Despite the efforts made to understand the switching mechanism using electron microscopy studies and physical models, key aspects of the filament formation such as the nucleation site and nature of the filament are still little known. The relatively fast relaxation process and the very small size of the filament make it hard to further conduct an in-depth physical analysis of the filament. Nonetheless, a valid qualitative conclusion can be drawn from the electrical measurement analyses, in combination with the observations from TEM studies.

In this regard, the first question to address is in which direction the filament retracts. To plot this, we investigated the directionality of the threshold switching. For the v-ECM cells to switch in both the negative and positive directions, there needs to be an active Ag ion source from both electrode sides. To examine this, the device was biased toward both positive and negative directions with varied I_{CC} under two different cases. In the first case, the device was formed at a low I_{CC} of 100 nA (to make sure it does not run into the non-volatile state). In the second case, the device was switched at a higher I_{CC} of 500 μA to drive it to a memory switching state. Then a subsequent negative voltage was applied to the Ag electrode to reset the device back to the HRS state. Then both devices were switched in a volatile manner. The results are shown in Figure S7. For the first case, volatile switching is observed only in the positively biased direction and the device remains in the HRS when biased in the negative direction (Figure S7b). From this, we can presume that the conductive filament retracts from the counter Pt electrode during the self-relaxation process. As a consequence, no switching is observed in the negative direction. However, for the second case, the device shows volatile switching in both positive and negative directions (Figure S7d). This suggests the existence of a residual Ag filament (Ag cluster) at the counter Pt electrode, which in turn acts as a local ion supply when a positive bias is applied to the Pt electrode. Therefore, for a controlled volatile switching, the retraction of the filament occurs at the counter electrode. This conclusion is consistent with TEM observations of filament breakage at the filament/inert electrode interface.[66]

The next is to address how much of the conductive filament retracts from the electrodes. In non-volatile ECMs, it is often the case that the current in the HRS state after the forming process is usually higher than that of the pristine device, mainly due to the incomplete rupture of the filament during the RESET process. As a result, a residual filament seed is left at the oxide/electrode interface.[85-87] However, v-ECM devices exhibit a very low leakage current,

almost similar to the pristine device, not only after forming but also repeated cycling (Figure 1d). Considering the ultra-thin HfO_2 layer thickness of 3 nm, a large portion of the conductive filament should retract from the electrodes to keep such ultra-low current. To evaluate this hypothesis, the tunneling current through the device was calculated by using Simmons model.[88] A conductive filament seed with a diameter of 5 nm is assumed as a residual filament (Figure S6). The tunneling current is calculated by accounting contributions from the whole device area with a fixed gap of 3 nm and through the residual filament by varying the tunneling gap accordingly. The result revealed that a tunneling gap of at least 2.0 nm is needed to keep the leakage current well below 100 fA (Figure S6b). This means that the conductive filament almost completely transformed into clusters by disconnecting from the electrodes during the relaxation process. A schematic of a possible switching mechanism for the unipolar and bipolar volatile switching is presented in Figure S7a and c, respectively.

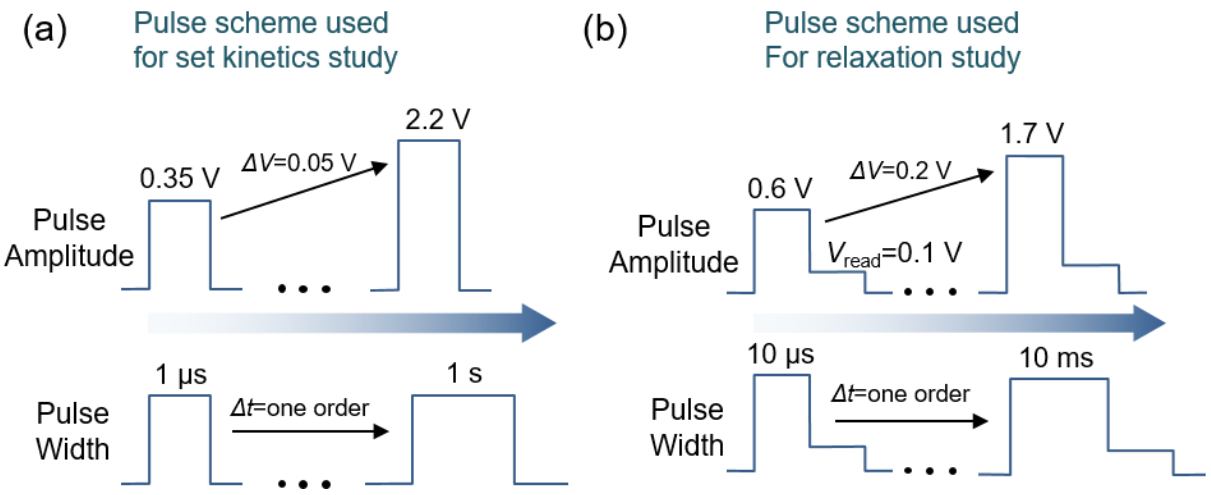

Figure S1. Schematic drawings showing the programming pulse schemes used to study a) the SET kinetics and b) the relaxation behavior.

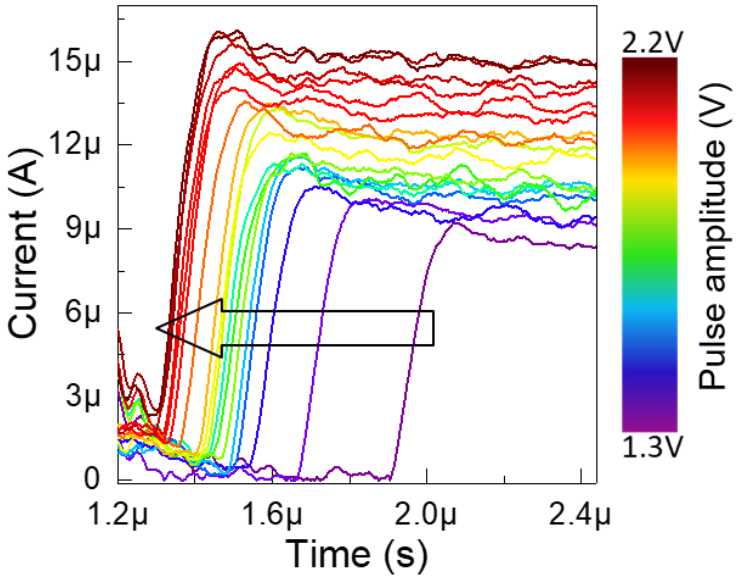

Figure S2. Typical I_{out}–t curve during the SET time measurement of the device under different V_p.

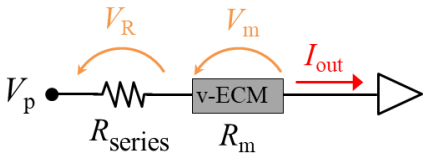

$$I_{total} = I_{out} = \frac{V_p}{R_{total}} \quad \text{(S1)}$$

$$R_{total} = R_{series} + R_m \quad \text{(S2)}$$

$$R_m = \left(\frac{V_p}{I_{out}}\right) - R_{series} \quad \text{(S3)}$$

$$V_R = \left(\frac{R_{series}}{R_{series}+R_m}\right) * V_p \quad \text{(S4)}$$

$$V_m = \left(\frac{R_m}{R_{series}+R_m}\right) * V_p \quad \text{(S5)}$$

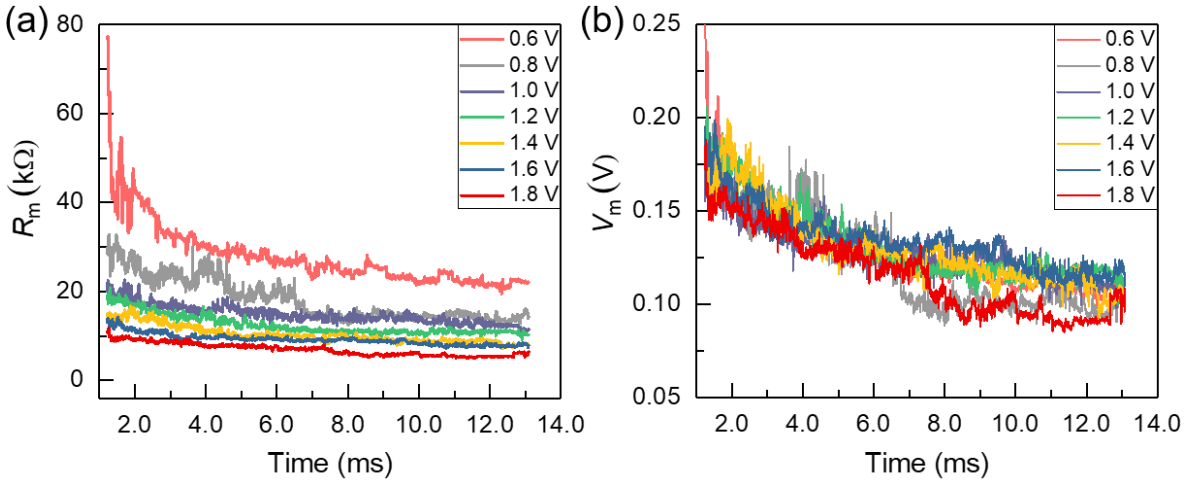

Figure S3. Resistance of the diffusive memristor (R_m) and the corresponding voltage drop (V_m) during the bias duration calculated by using equation S3 and S5.

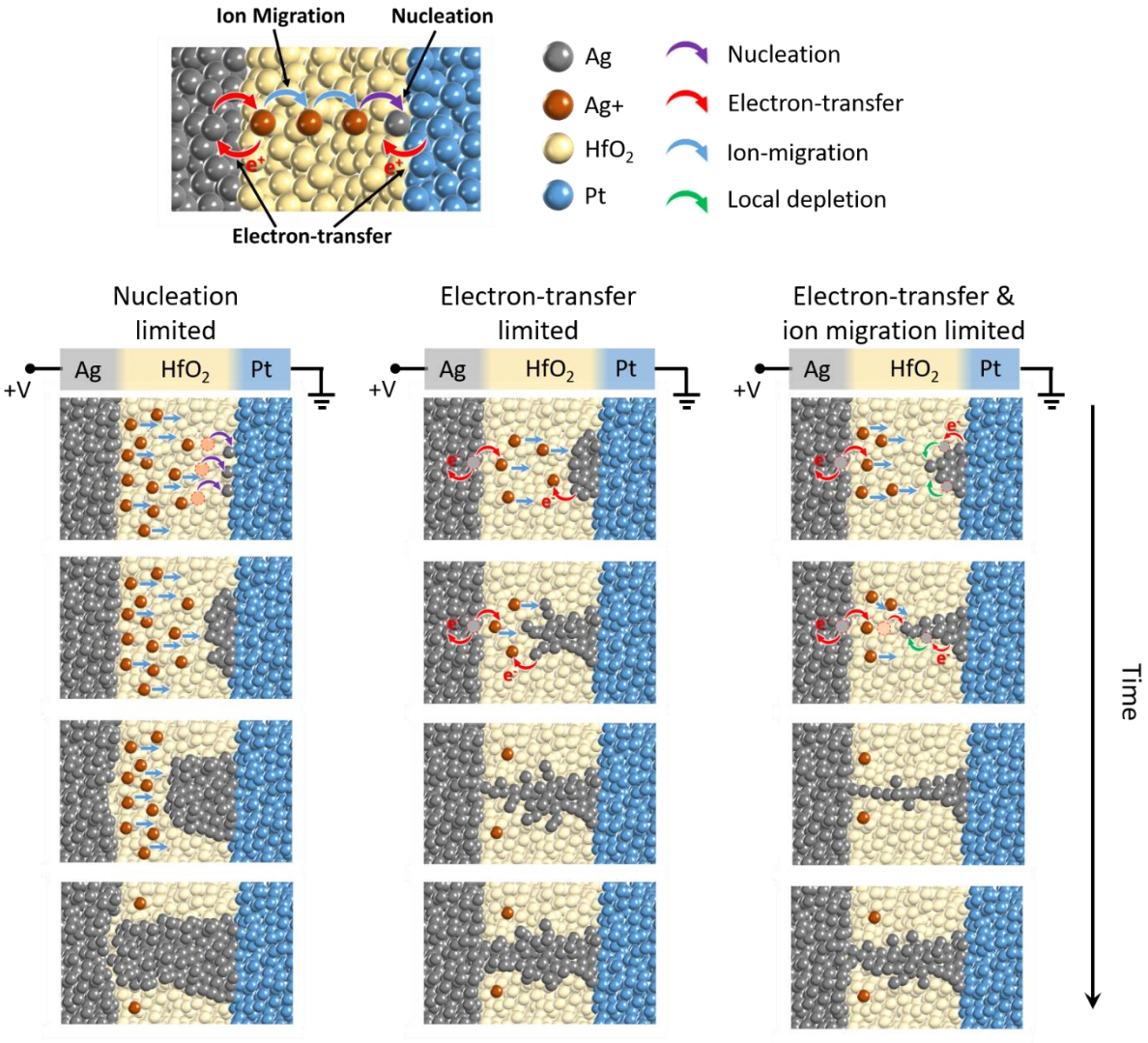

Figure S4. Voltage-dependent filament growth mechanisms. At low voltages where nucleation is the limiting step, a homogenous growth and a relatively bulky filament are expected. In the intermediate region where electron transfer limits the filament's growth rate, a linear growth of a dendritic-shaped filament occurs. At higher voltages where ion-migration also becomes the limiting factor, local depletion of Ag ion creates a field enhancement effect in the filament region. This causes a self-accelerated and anisotropic growth and eventually, a thin filament is formed.

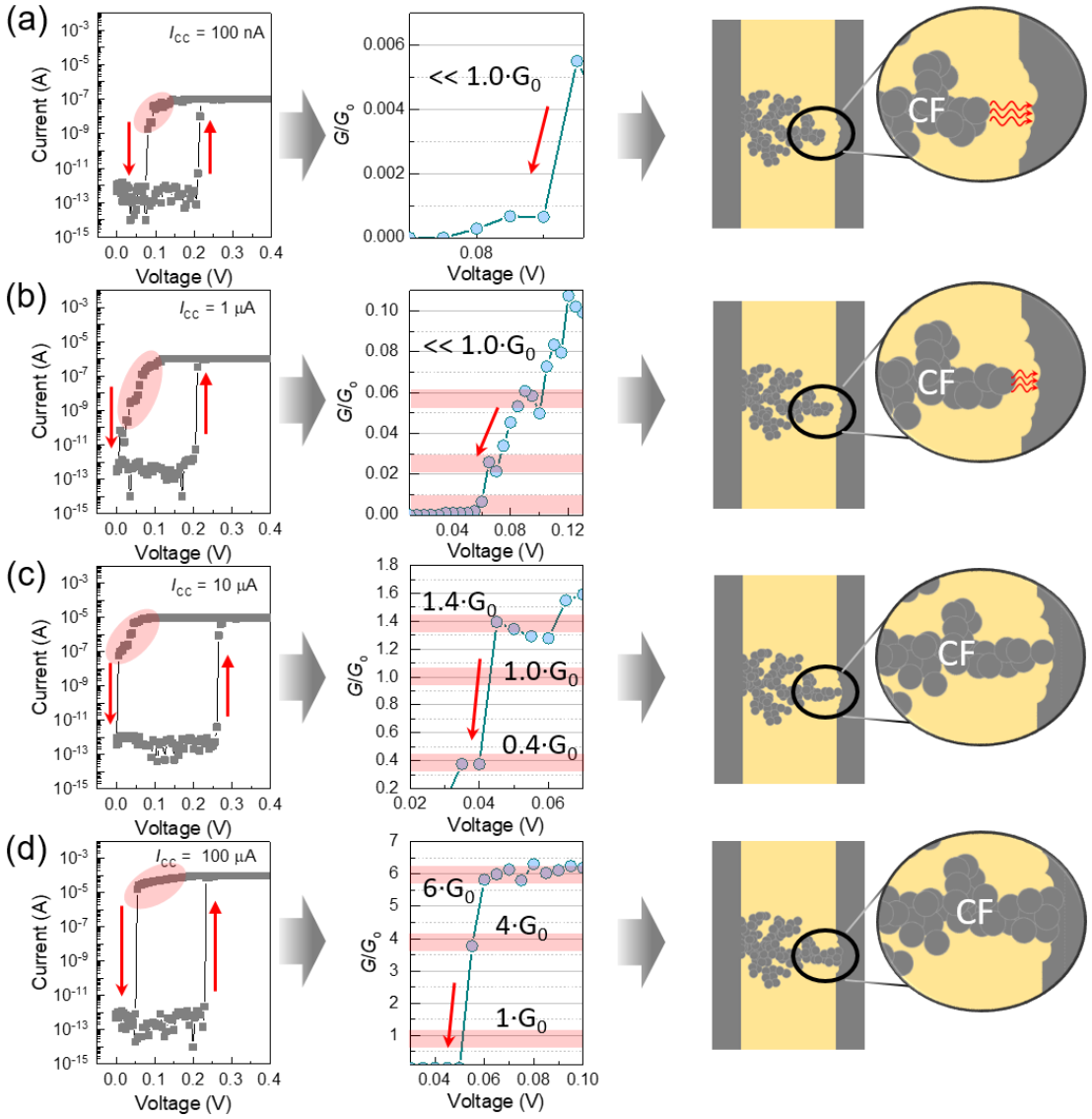

Figure S5. Sweep measurement under different compliance currents and the corresponding conductance values. The plots on the right are a schematic representation of the filament evolutions under various compliance currents.

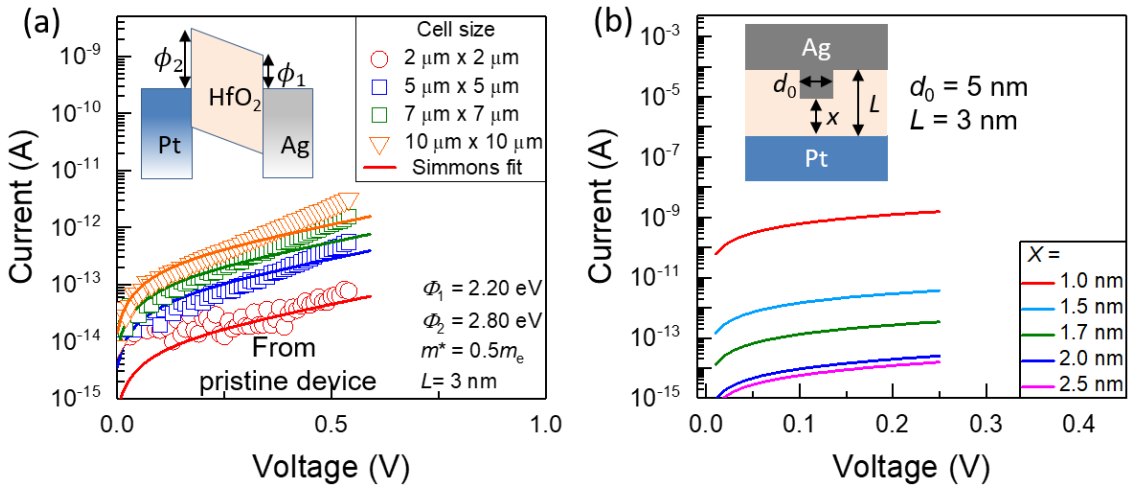

Figure S6. (a) Simmons fitting of leakage current curves of pristine devices for various cell sizes. (b) Tunneling currents calculated using Simmons model with different tunneling gaps.

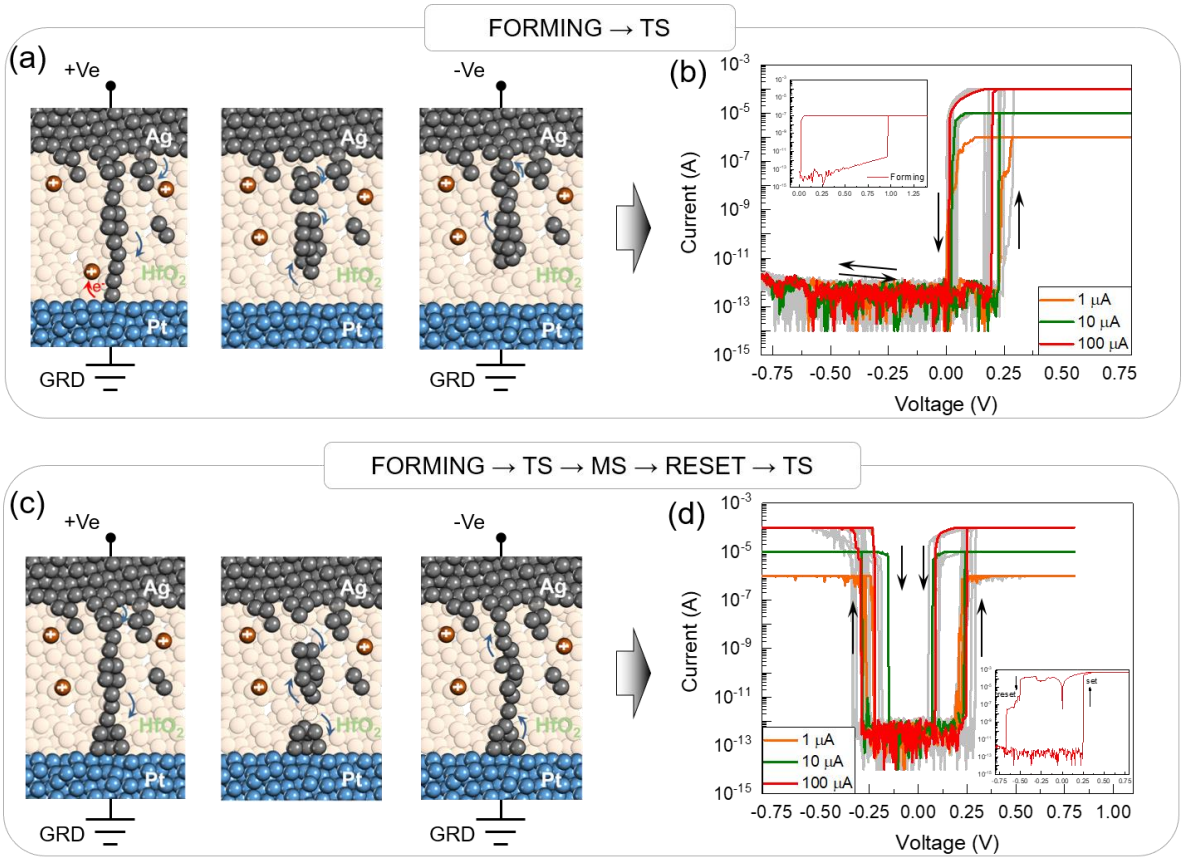

Figure S7. Schematic representation of switching mechanism in v-ECM under unipolar a) and bipolar mode c). Respective *I-V* sweeps are shown in b) and d), respectively. Inset in b) shows the first forming step. Inset in d) displays the SET and RESET processes of the cell in the non-volatile mode.

References

[1] Y. Yang, P. Gao, S. Gaba, T. Chang, X. Pan, W. Lu, *Nature Communications* **2012**, *3*, 732.

[2] S. Z. Rahaman, S. Maikap, W. S. Chen, H. Y. Lee, F. T. Chen, T. C. Tien, M. J. Tsai, *J. Appl. Phys.* **2012**, *111*, 63710/1.

[3] D. Kumar, R. Aluguri, U. Chand, T. Y. Tseng, *Appl. Phys. Lett.* **2017**, *110*, 203102/1.

[4] M. Barci, G. Molas, C. Cagli, E. Vianello, M. Bernard, A. Roule, A. Toffoli, J. Cluzel, B. De Salvo, L. Perniola, *IEEE J. Electron Devices Soc.* **2016**, *4*, 314.

[5] J. G. Simmons, *J. Appl. Phys.* **1963**, *34*, 1793.